

Reshaping the Tips of ZnO Nanowires by Pulsed Laser Irradiation

Xue Wang^{1,2,§}, Yong Ding^{1,§}, Dajun Yuan³, Jung-Il Hong¹, Yan Liu¹, C. P. Wong¹, Chenguo Hu², and Zhong Lin Wang¹ (✉)

¹ School of Materials Science and Engineering, Georgia Institute of Technology, Atlanta, Georgia 30332, USA

² Department of Applied Physics, Chongqing University, Chongqing 400044, China

³ Woodruff School of Mechanical Engineering, Georgia Institute of Technology, Atlanta, Georgia 30332-0405, USA

[§] These authors contributed equally to this work.

Received: 3 March 2012 / Revised: 3 April 2012 / Accepted: 24 April 2012

© Tsinghua University Press and Springer-Verlag Berlin Heidelberg 2012

ABSTRACT

Vertically aligned ZnO nanowires have been synthesized by a hydrothermal method. After being irradiated by a short laser pulse, the tips of the as-synthesized ZnO nanowires can be tailored into a spherical shape. Transmission electron microscopy revealed that the spherical tip is a single-crystalline piece connected to the body of the ZnO nanowire, and that the center of the sphere is hollow. The growth mechanism of the hollow ZnO nanospheres is proposed to involve laser-induced ZnO evaporation immediately followed by re-nucleation in a temperature gradient environment. The laser-irradiated ZnO nanowire array shows hydrophobic properties while the original ZnO nanowire array shows hydrophilicity. The as-grown ZnO nanowire arrays with hollow spherical tips can serve as templates to grow ZnO nanowire arrays with very fine tips, which may be a good candidate material for use in field emission and scanning probe microscopy.

KEYWORDS

ZnO nanowires, laser irradiation, hollow ZnO nanospheres, surface wettability, fine ZnO tips

1. Introduction

Engineering and shape-controlled growth of high-quality nanostructures is challenging, but very useful for realizing special nanostructure-induced properties [1–3]. For example, surface wettability can be modified by changing straight nanowire (NW) arrays into bent NW arrays [4, 5], and field emission can be enhanced by engineering nanotips on ZnO nanobottles [6].

As a wide direct band-gap (~3.37 eV) semiconductor, ZnO has versatile applications in self-powered devices

and nanogenerators [7, 8], light-emitting diodes [9], solar cells [10], gas sensors [11], and many other areas. A lot of work has been done to produce useful ZnO nanostructures with various morphologies (including nanowires [8], nanotubes [10, 12], nanorings [13], and nanospheres [14]), and several strategies have been developed for further modification of the shapes of these post-growth nanostructures. Shen et al. [15] reported that bent ZnO NWs with a desired shape can be obtained by depositing a secondary material sideways using pulsed laser deposition (PLD). Cheng

Address correspondence to zlwang@gatech.edu

et al. [6] and Xu et al. [16] reported that ZnO nanotips can be decorated on pre-existing ZnO nanostructures by re-growth of the latter. Hollow ZnO nanostructures are of particular interest due to their lower densities and higher surface areas, which lead to potential applications as capsule agents for drug delivery, or templates for functional-architected composite materials [17, 18]. Normally, hollow ZnO nanostructures are obtained by chemical etching or template-assisted synthesis [18–21], but single-crystalline spherical ZnO nanostructures are usually very difficult to fabricate by these methods. So it would be challenging but interesting to seek simpler and more effective processes for the synthesis of hollow spherical single-crystalline ZnO nanostructures.

In this work, we report a simple strategy for fabricating single-crystal ZnO hollow nanospheres (HNSs) at the tips of pre-synthesized ZnO NWs by using pulsed laser irradiation. Based on the structure of the HNSs, a growth mechanism has been proposed. Furthermore, the laser-irradiated ZnO NW array showed hydrophobic properties, in contrast to the hydrophilic behavior of the as-grown ZnO NW array. Furthermore, by re-growth of the laser-irradiated ZnO NWs, fine ZnO nanotips can be decorated on the tops of the ZnO HNSs which may greatly enhance the field emission of the as-synthesized samples.

2. Experimental

2.1 Chemical synthesis of well-aligned ZnO nanowire arrays

Vertically aligned ZnO NW arrays were synthesized by a simple hydrothermal method [22]. In brief, a fluorine-doped SnO₂ (FTO) glass substrate (2 cm × 2 cm) was rinsed ultrasonically, successively in acetone, ethanol, and distilled water. After that, a ZnO seed layer (50 nm in thickness) was deposited on the conductive surface of the as-prepared FTO glass by a thermal evaporator (a 200 nm polycrystalline ZnO thin film was also obtained by this method). Then the substrate was immersed in a mixed solution consisting of equimolar (0.02 mol/L) zinc chloride (ZnCl₂) and hexamethylenetetramine (HMTA, (CH₂)₆N₄) with a small amount of ammonium hydroxide (NH₃, 28%, 5 mL in 100 mL solution), and heated at 85 °C for 8 h.

Finally, the sample was cooled down to room temperature naturally and thoroughly washed by ethanol and deionized water.

2.2 Pulsed laser irradiation of ZnO nanowires

The as-synthesized ZnO NW array was mounted on a target which was ~50 cm away from the laser source and ablated by one short pulse of a KrF excimer laser (wavelength 248 nm, pulse time = 25 ns, energy per pulse = 210 mJ, energy density = 230 mJ·cm⁻²) directly from its top side. The laser ablation was performed in an ambient environment at room temperature.

2.3 Chemical synthesis of fine ZnO nanotips

The laser-irradiated ZnO NW array was immersed in a mixed solution of 5 mmol/L ZnCl₂ and 5 mmol/L HMTA, and first heated at 85 °C for 2 h and subsequently followed by heating at 65 °C for 4 h. After that, the sample was cooled down to room temperature naturally and thoroughly washed by ethanol and deionized water.

2.4 Instruments and measurements

A pulsed UV laser beam was emitted from a Coherent Complex 205 KrF excimer laser source. Scanning electron microscopy (SEM) was performed using a Leo 1550 scanning electron microscope at 5 kV. High-resolution transmission electron microscopy (HRTEM) and energy-dispersive X-ray spectroscopy (EDS) results were obtained from a JEOL 4000EX and a Hitachi HF-2000 transmission electron microscope. Water contact angle measurements were performed with a Ramé-Hart goniometer that had an attached Charge-coupled Device (CCD) camera equipped for image capture. The deionized water droplet volume was 4 μL, and the measurements were obtained under ambient atmospheric conditions.

3. Results and discussion

Vertically aligned ZnO NWs with uniform size of around 3.6 μm in length and 150 nm in diameter (Fig. 1(a) and its inset) were synthesized by a hydrothermal method. The as-synthesized ZnO NW array was mounted in an ambient environment



approximately 50 cm away from the laser source, and was then irradiated by one short pulse of a KrF excimer laser directly from its top side. Dramatic changes were observed after laser irradiation. All tips of the NWs changed into a spherical shape, as shown in Fig. 1(b). The modified ZnO NWs were further investigated by transmission electron microscopy (TEM) and EDS. As shown in Fig. 2(a), the cross-section of the original nanowire had a hexagonal shape (Fig. 2(a) inset, top left corner), which is the standard morphology of ZnO NWs. What is interesting is that hollow ZnO nanospheres (Fig. 2(a) inset, bottom right corner) can be obtained on the tips of these NWs after laser irradiation, which indicates that the formation of the spherical tips not only includes simple melting and

cooling processes of the target material, but also the formation of new nanostructures. The insets of Fig. 2(a) show the selected area electron diffraction (SAED) patterns of the ZnO HNS and the original ZnO NW. It is noteworthy that a hollow ZnO nanosphere still has a single-crystal structure, showing that a rapid crystallization occurred during the re-growth procedure. Moreover, traditional ZnO single crystals grown by a gradual procedure usually have a hexagonal shape. A spherical hollow single-crystalline ZnO nanostructure is rare, and the mechanism of its formation will be discussed below. EDS analysis results acquired from the spherical area (red curve) and nanowire region (black curve) in Fig. 2(a) are displayed in Fig. 2(b), indicating that these two areas

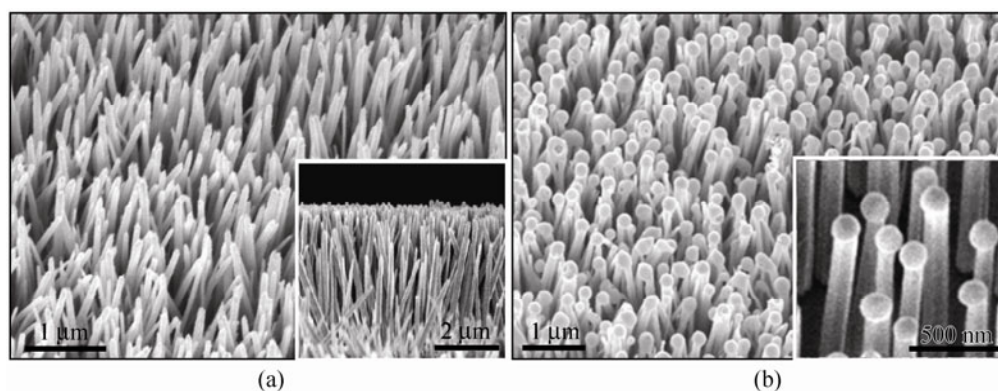


Figure 1 Morphology change of the as-grown ZnO NW arrays before and after laser irradiation. (a) 30°-tilted-view and side-view (inset) SEM images of the as-synthesized ZnO NW array. (b) 30°-tilted-view SEM images of the as-synthesized ZnO NW array after pulsed laser irradiation with a fluence of $230 \text{ mJ}\cdot\text{cm}^{-2}$

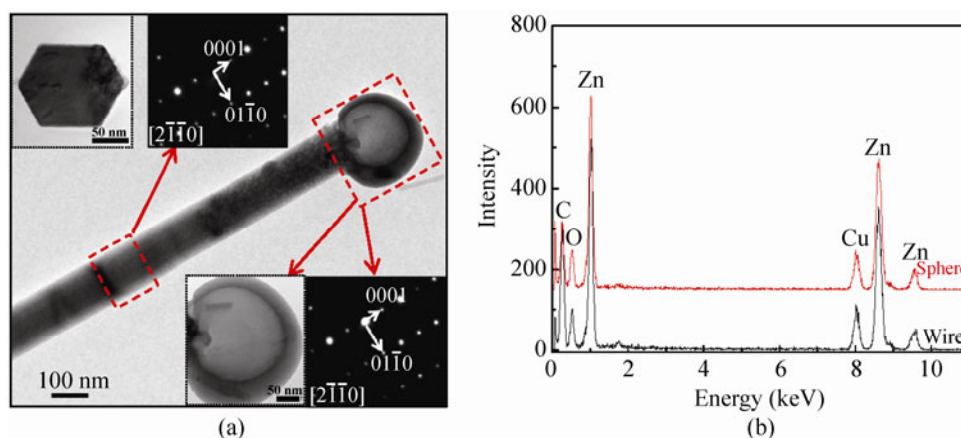


Figure 2 Single-crystal structure nature of the ZnO hollow sphere formed at the tip. (a) TEM image of a laser-irradiated ZnO NW, with the insets showing the SAED patterns of the wire region and the spherical tip. The inset image at the top-left hand side is a cross-section TEM image from a NW, showing its hexagonal shape. (b) EDS results obtained from the wire region (black curve) and the spherical tip (red curve)

have similar Zn/O ratios (Cu and C signals are from the TEM grid). In other words, significant oxygen loss did not occur during the formation of our ZnO HNSs because the laser process was carried out in an ambient environment which promotes re-combination of Zn^{2+} and O^{2-} ions.

Observation from different lattice planes is helpful in studying the detailed structure of ZnO nanocrystals. To this end, we embedded the laser-irradiated ZnO NWs in epoxy and used an ultramicrotome to cut the ZnO HNSs along different directions. HRTEM was utilized for analysis of the obtained slices (40 nm in thickness) to further study the structure of our ZnO HNSs. Figures 3(a)–3(c) show HRTEM images of a ZnO HNS cut along the c -plane, from which we can see that the ZnO HNS has a shell of about 35 nm in thickness (Fig. 3(a)) and a smooth surface (Fig. 3(b)). The image in Fig. 3(c) taken from the central region in Fig. 3(a) (as marked by the red rectangle) shows that the atoms in the c -plane are well-arranged one by one, and no obvious oxygen or zinc vacancies are observed. Figures 3(d)–3(f) show HRTEM images of another ZnO HNS cut perpendicular to the c -plane.

The image acquired from the middle region in Fig. 3(d), shown in Fig. 3(f), confirms that the number of oxygen vacancies is small, further demonstrating the good re-combination of Zn^{2+} and O^{2-} ions during the formation of ZnO HNSs.

Although Lee's group has reported that excimer laser annealing can introduce morphology changes of ZnO NWs [23], only solid spherical tips were observed and a detailed mechanism for the formation of the spherical ZnO nanostructures was not proposed. We illustrate the processes involved in the formation of our ZnO HNSs in Fig. 4. As is well known, the effect of laser irradiation can be ascribed mainly to the thermal effect caused by the absorption of excimer laser energy. Szorenyi et al. [24] have simulated the temperature profiles of indium tin oxide (ITO) thin films on a glass substrate after a single pulse of KrF excimer laser irradiation, and similar temperature changes may be expected to take place in the presence of ZnO NWs. From their work, we can infer that, when irradiated with a laser fluence of $230 \text{ mJ}\cdot\text{cm}^{-2}$, the surface temperature of ZnO NWs can rise to $\sim 2400 \text{ K}$ which is higher than the melting point of ZnO (2248 K). What is

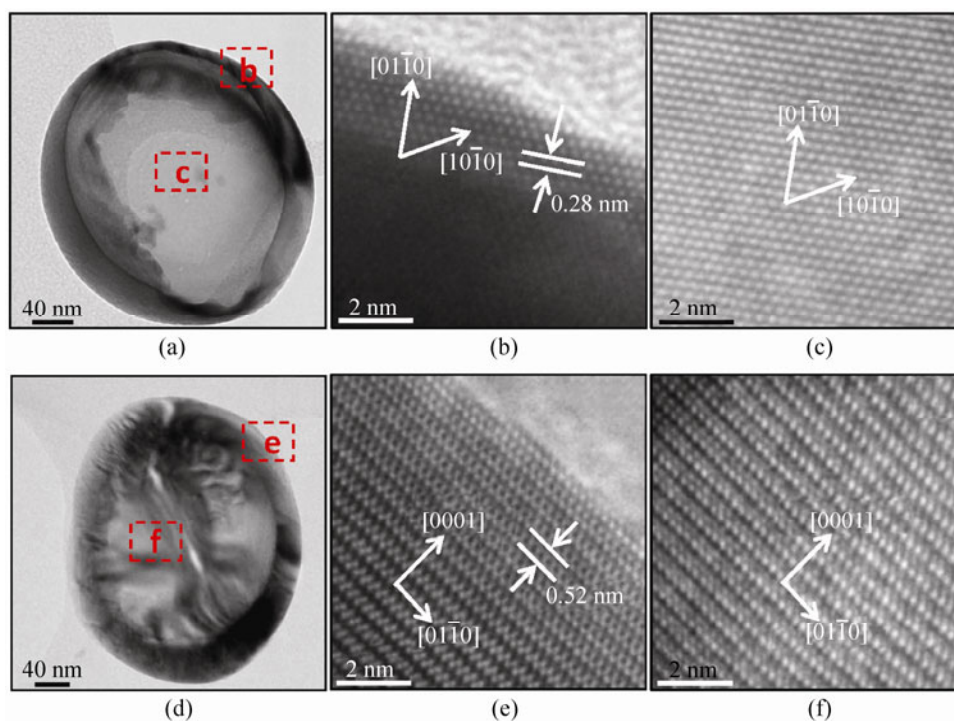


Figure 3 TEM and HRTEM images of a ZnO HNS cut (a)–(c) along the c -axis and (d)–(f) perpendicular to the c -axis to illustrate the single-crystal structure of the hollow shell

more, the photon energy of the KrF excimer laser used here ($479.6 \text{ kJ}\cdot\text{mol}^{-1}$) is high enough to break the Zn–O bonds ($248 \text{ kJ}\cdot\text{mol}^{-1}$) [25]. By mass spectrometry and photoionization studies of the ablation of ZnO with a 248 nm KrF excimer laser, Leuchtner found that the most prominent ejected species were monatomic Zn and O atoms and their ions [26]. So in our case, as shown in Fig. 4(b), a short and strong laser pulse with a fluence of $230 \text{ mJ}\cdot\text{cm}^{-2}$ heated the ZnO within the laser irradiation region and melted it into a cluster cloud of Zn, O, Zn^{2+} and O^{2-} . When the heating procedure was continued, more raw ZnO NWs were depleted and the cloud volume increased (Fig. 4(c)). Subsequently, once the laser pulse was switched off, ambient cooling air (represented by arrows in Fig. 4(d))

around the sample caused a sharp temperature gradient from the surface to the center of the ejected species (Fig. 4(d)) and introduced a cooling and shrinking of the cluster cloud (Fig. 4(e)). Because ejected species at the outer side were cooled down most rapidly due to rapid heat exchange, and the remaining NW can serve as a nucleation site there, the first re-crystallization and epitaxial growth step was realized at the outermost region closest to the top of the remaining NW (Fig. 4(f)), and subsequently the outer clusters further away from the NW re-crystallized. As the nucleation continued, a closed shell formed (Fig. 4(g)) and its inner surface acted as a new nucleation site for absorbing encircled clusters onto its inside wall, resulting in re-crystallization (Fig. 4(h)). After exhausting all of the

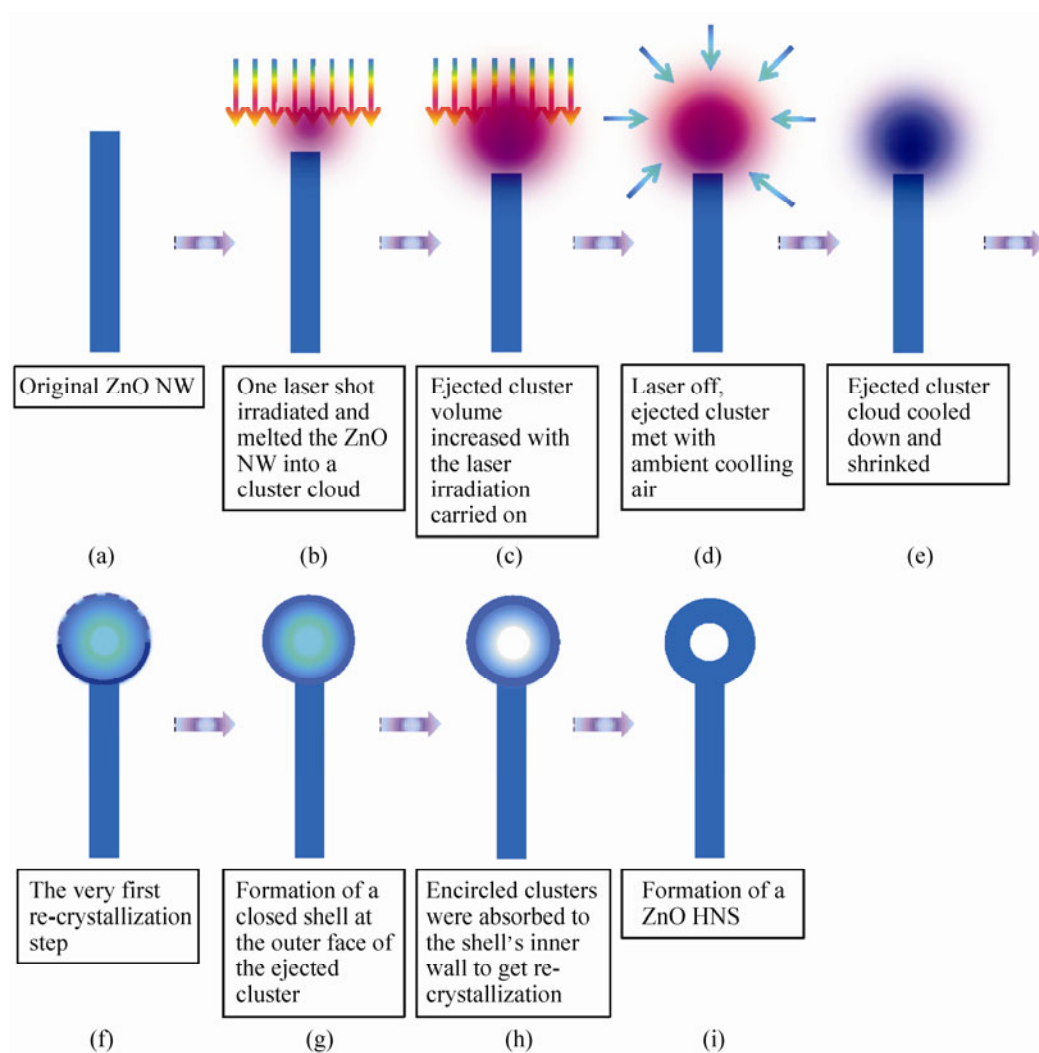


Figure 4 Schematic illustration of the processes involved in the formation of the ZnO HNSs

vapor phase, there will be a hollow inside the sphere, which may be under vacuum due to the shrinkage and disappearance of the “gas” type species. Finally, a ZnO HNS formed on the top of the corresponding ZnO NW (Fig. 4(i)).

To further study the mechanism of formation of our ZnO HNSs, several supplementary experiments were carried out. All of the experiments were performed under the same conditions as discussed above except that different laser fluences were used to irradiate the target material. When irradiated by one pulse of low fluence laser ($70 \text{ mJ}\cdot\text{cm}^{-2}$), no change could be observed on the tops of the ZnO NWs (Fig. 5(a) and 5(b)), because the laser power was too weak to induce a high enough surface temperature to melt the ZnO NWs. However, when irradiated with one laser pulse of high energy density ($1750 \text{ mJ}\cdot\text{cm}^{-2}$), a huge amount of heat was introduced and caused more ejections and a wider diffusion of ejected species. As a result, clusters formed by adjacent NWs mixed with each other, and finally formed an irregular surface coating on the remaining NWs after cooling (Fig. 5(c)). As for a polycrystalline ZnO thin film (Fig. 5(d), 200 nm in thickness), after irradiation with one laser pulse with a fluence of $230 \text{ mJ}\cdot\text{cm}^{-2}$, no ZnO HNSs were formed, and a porous re-crystallized thin film was found

instead (Fig. 5(e)). This is because fine ZnO crystals were well-distributed on the substrate surface and, when irradiated by a laser pulse, ejected species became distributed nearly uniformly on top of the target material instead of forming several isolated cluster clouds. Furthermore, nucleation sites exist randomly on the remaining thin film. As a result, during the cooling procedure, a porous re-crystallized ZnO thin film with an irregular shape was obtained on top of the target thin film. Based on above discussions, we can conclude that irradiation with a suitable laser fluence and isolated ZnO NWs are both required for formation of ZnO HNSs.

As a novel nanostructure of single-crystalline ZnO, the specific properties and applications of the hollow ZnO nanospheres are of considerable interest. Herein, we have demonstrated the changes in surface wettability of a ZnO NW array before and after laser irradiation and the results are shown in Figs. 6(a) and 6(b). From these two figures we can see that the as-grown ZnO NW array was originally hydrophilic with a water contact angle of 20° (Fig. 6(a)). However, after laser irradiation with a fluence of $230 \text{ mJ}\cdot\text{cm}^{-2}$, the material surface displayed water-repellent properties (with a water contact angle of 120° , shown in Fig. 6(b)). This change in surface wettability must be due to the

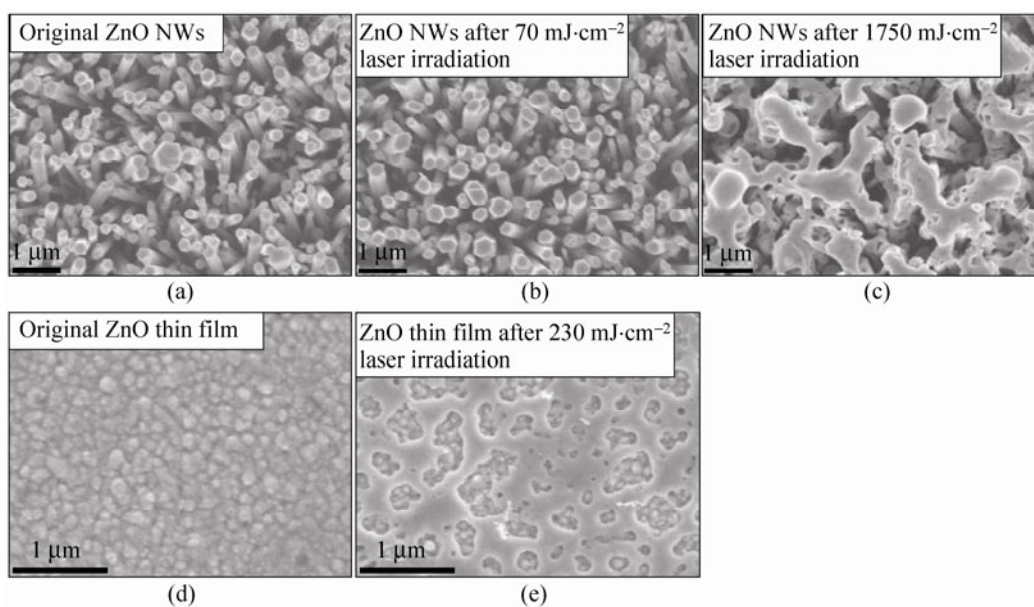


Figure 5 Top-view SEM images of (a) the original ZnO NWs, and the original ZnO nanowires after laser irradiation with a fluence of (b) $70 \text{ mJ}\cdot\text{cm}^{-2}$ and (c) $1750 \text{ mJ}\cdot\text{cm}^{-2}$. Top-view SEM images of a polycrystalline ZnO thin film (d) before and (e) after laser irradiation with a fluence of $230 \text{ mJ}\cdot\text{cm}^{-2}$

change in ZnO surface energy induced by laser irradiation. It is well known that nanostructures with low surface energies can prevent the penetration of water and lead to a high contact angle. In contrast, nanostructures with high surface energies exhibit hydrophilicity due to the nanowicking of water into the nanostructure via three-dimensional capillaries [27–29]. For ZnO, the {0001} plane is a polar surface with a higher surface energy than the other planes [30, 31]. From the TEM results shown in Fig. 2(a) we can see that the as-fabricated ZnO NWs grew along the *c*-axis and kept the *c*-plane exposed at their ends. But after irradiation by a laser pulse, the NW tips changed into a spherical shape with a very tiny

exposure of *c*-planes. That is to say, laser irradiation can modify the exposed area of the *c*-plane of ZnO and consequently cause a reduction in surface energy. As a result, the ZnO NW array changed from a hydrophilic surface to a hydrophobic one. This result indicates that laser irradiation may become a new effective way to change the surface wettability of ZnO nanostructures, in addition to the traditional way of surface modification by an appropriate chemical reagent [27–29]. In addition, based on the tiny exposure of *c*-planes, a sub-ZnO nanostructure synthesis procedure was carried out using the ZnO HNSs as templates. This growth was enabled by a two-step hydrothermal method, with growth temperatures of

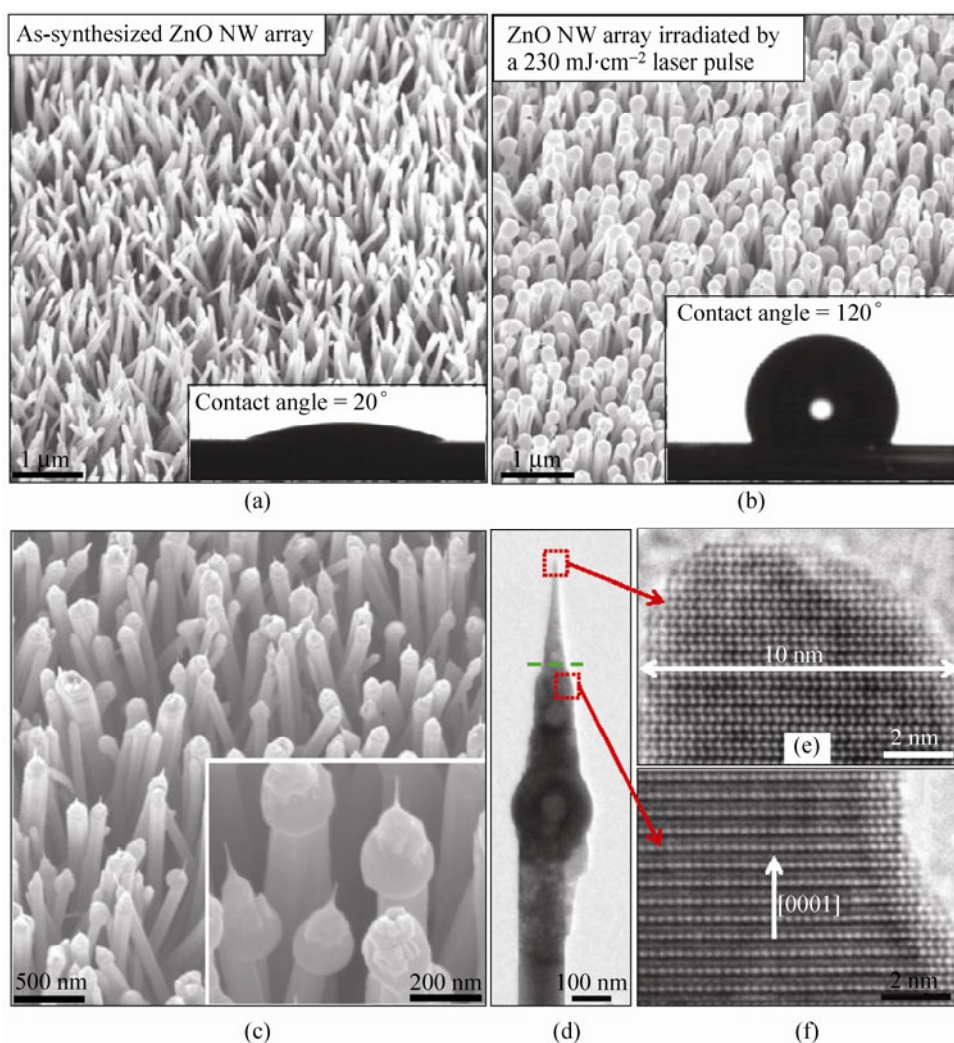


Figure 6 SEM images and measured water contact angles of a ZnO NW array (a) before and (b) after laser irradiation with a fluence of $230 \text{ mJ}\cdot\text{cm}^{-2}$. (c) 30° -tilted-view SEM and (d) TEM images of a laser-irradiated ZnO NW array after the formation of nanotips by re-growth. HRTEM images taken from (e) the end and (f) the edge area of the fine ZnO nanotip

85 °C for the first 2 h and 65 °C for the next 4 h. It is impressive that fine ZnO nanotips were obtained on the tops of ZnO HNSs after this secondary growth, as shown in Fig. 6(c). The boundary between the two growth steps can be easily found in the TEM image (marked by a green dashed line in Fig. 6(d)). As previously reported for ZnO NWs, sub-ZnO nanostructures always favor epitaxial growth from pre-existing ZnO structures in order to reduce system energy, interface strain and lattice mismatch [6, 16, 32]. Thus, the tiny *c*-plane on the top of the ZnO HNS can easily enable the growth of sub-ZnO nanostructures on it. Because the diameters of these new nanostructures strongly depend on the areas of the nucleation sites provided by the precursors, the very tiny area of the *c*-plane on the ZnO HNS can help to induce secondary ZnO nanotips with a very small diameter. Moreover, because ZnO NWs will not only grow along their length direction, but also have a lateral expansion, it is difficult to get very fine NWs from a one-step synthesis. In our two-step growth method used here, the tiny *c*-plane on the top resulting from the first growth step will further act as the template for the second step to promote the formation of extremely fine nanotips.

As we can see from Fig. 6(d), the first synthesis step resulted in a nanotip with a larger diameter. Subsequently, a lower temperature growth procedure took place, and a fine tip grew from the *c*-plane top formed by the first step. From HRTEM images of the top (Fig. 6(e)) and edge region (Fig. 6(f)) of the nanotip shown in Fig. 6(d), we can find that the fine ZnO nanotip is well crystallized and also grows along the *c*-axis. What is more, the diameter at the end of the nanotip can be as small as 10 nm which gives huge potential improvements in the field-emission performance of the resulting material.

4. Conclusions

We have developed an effective method to synthesize single-crystalline hollow ZnO nanospheres. The growth mechanism of these ZnO HNSs has been proposed to involve laser-induced ZnO evaporation followed by re-nucleation in a temperature gradient environment. Moreover, because of the tiny exposed area of the *c*-plane of the ZnO HNSs, the surface wettability of

the ZnO NW array can be changed from the original hydrophilic to hydrophobic, and fine ZnO nanotips can be obtained on the tops of the HNSs after a re-growth procedure, which may result in dramatic improvements in the field-emission performance of our ZnO NWs.

Acknowledgements

This research was supported by Basic Energy Sciences (BES), Department of Energy (DOE) and National Science Foundation (NSF). X. Wang and C. G. Hu acknowledge the support of NSFC (60976055) and the Postgraduates' Science and Innovation Fund (201005B1A0010339) of Chongqing University. X. Wang also would like to acknowledge the fellowship from the China Scholarship Council (CSC) (2010605070).

References

- [1] Sun, T. L.; Feng, L.; Gao, X. F.; Jiang, L. Bioinspired surfaces with special wettability. *Acc. Chem. Res.* **2005**, *38*, 644–652.
- [2] Autumn, K. Gecko adhesion: Structure, function, and applications. *MRS Bull.* **2007**, *32*, 473–478.
- [3] Kim, T. I.; Jeong, H. E.; Suh, K. Y.; Lee, H. H. Stoooped nanohairs: Geometry-controllable, unidirectional, reversible, and robust gecko-like dry adhesive. *Adv. Mater.* **2009**, *21*, 2276–2281.
- [4] Kim, T. I.; Suh, K. Y. Unidirectional wetting and spreading on stoooped polymer nanohairs. *Soft Matter* **2009**, *5*, 4131–4135.
- [5] Chu, K. H.; Xiao, R.; Wang, E. N. Uni-directional liquid spreading on asymmetric nanostructured surfaces. *Nat. Mater.* **2010**, *9*, 413–417.
- [6] Cheng, C. L.; Chao, S. H.; Chen, Y. F. Enhancement of field emission in nanotip-decorated ZnO nanobottles. *J. Cryst. Growth* **2009**, *311*, 4381–4384.
- [7] Xu, S.; Qin, Y.; Xu, C.; Wei, Y. G.; Yang, R. S.; Wang, Z. L. Self-powered nanowire devices. *Nat. Nanotechnol.* **2010**, *5*, 366–373.
- [8] Zhu, G. A.; Yang, R. S.; Wang, S. H.; Wang, Z. L. Flexible high-output nanogenerator based on lateral ZnO nanowire array. *Nano Lett.* **2010**, *10*, 3151–3155.
- [9] Lupan, O.; Pauporte, T.; Viana, B. Low-voltage UV-electroluminescence from ZnO-nanowire array/p-GaN light-emitting diodes. *Adv. Mater.* **2010**, *22*, 3298–3302.
- [10] Han, J. B.; Fan, F. R.; Xu, C.; Lin, S. S.; Wei, M.; Duan, X.; Wang, Z. L. ZnO nanotube-based dye-sensitized solar cell



- and its application in self-powered devices. *Nanotechnology* **2010**, *21*, 405203.
- [11] Comini, E.; Faglia, G.; Sberveglieri, G.; Pan, Z. W.; Wang, Z. L. Stable and highly sensitive gas sensors based on semiconducting oxide nanobelts. *Appl. Phys. Lett.* **2002**, *81*, 1869–1871.
- [12] Xi, Y.; Song, J. H.; Xu, S.; Yang, R. S.; Gao, Z. Y.; Hu, C. G.; Wang, Z. L. Growth of ZnO nanotube arrays and nanotube based piezoelectric nanogenerators. *J. Mater. Chem.* **2009**, *19*, 9260–9264.
- [13] Kong, X. Y.; Ding, Y.; Yang, R.; Wang, Z. L. Single-crystal nanorings formed by epitaxial self-coiling of polar-nanobelts. *Science* **2004**, *303*, 1348–1351.
- [14] Matsumoto, K.; Saito, N.; Mitate, T.; Hojo, J.; Inada, M.; Haneda, H. Surface polarity determination of ZnO spherical particles synthesized via solvothermal route. *Cryst. Growth Des.* **2009**, *9*, 5014–5016.
- [15] Shen, Y.; Hong, J. I.; Xu, S.; Lin, S. S.; Fang, H.; Zhang, S.; Ding, Y.; Snyder, R. L.; Wang, Z. L. A general approach for fabricating arc-shaped composite nanowire arrays by pulsed laser deposition. *Adv. Funct. Mater.* **2010**, *20*, 703–707.
- [16] Xu, H. J.; Hou, Y. M.; Gao, J. Y.; Zhu, H. C.; Zhu, R.; Sun, Y. H.; Zhu, X. L.; Wang, Y. Z.; Wang, X. W.; Yu, D. P. Regrowth of template ZnO nanowires for the underlying catalyst-free growth mechanism. *Cryst. Growth Des.* **2011**, *11*, 2135–2141.
- [17] Elias, J.; Levy-Clement, C.; Bechelany, M.; Michler, J.; Wang, G. Y.; Wang, Z.; Philippe, L. Hollow urchin-like ZnO thin films by electrochemical deposition. *Adv. Mater.* **2010**, *22*, 1607–1612.
- [18] Zeng, H. B.; Cai, W. P.; Liu, P. S.; Xu, X. X.; Zhou, H. J.; Klingshirn, C.; Kalt, H. ZnO-based hollow nanoparticles by selective etching: Elimination and reconstruction of metal-semiconductor interface, improvement of blue emission and photocatalysis. *ACS Nano* **2008**, *2*, 1661–1670.
- [19] Liu, J.; Chen, X. L.; Wang, W. J.; Huang, Q. S.; Wang, G.; Zhu, K. X.; Guo, J. G. Large scale synthesis of porous ZnO hollow structures with tunable diameters and shell thicknesses. *Mater. Lett.* **2009**, *63*, 2221–2223.
- [20] Park, J. Y.; Choi, S. W.; Kim, S. S. A synthesis and sensing application of hollow ZnO nanofibers with uniform wall thicknesses grown using polymer templates. *Nanotechnology* **2010**, *21*, 475601.
- [21] Zhang, Z. Y.; Li, X. H.; Wang, C. H.; Wei, L. M.; Liu, Y. C.; Shao, C. L. ZnO hollow nanofibers: Fabrication from facile single capillary electrospinning and applications in gas sensors. *J. Phys. Chem. C* **2009**, *113*, 19397–19403.
- [22] Gao, Y. F.; Nagai, M.; Chang, T. C.; Shyue, J. J. Solution-derived ZnO nanowire array film as photoelectrode in dye-sensitized solar cells. *Cryst. Growth Des.* **2007**, *7*, 2467–2471.
- [23] Maeng, J.; Heo, S.; Jo, G.; Choe, M.; Kim, S.; Hwang, H.; Lee, T. The effect of excimer laser annealing on ZnO nanowires and their field effect transistors. *Nanotechnology* **2009**, *20*, 095203.
- [24] Szorenyi, T.; Laude, L. D.; Bertoti, I.; Kantor, Z.; Geretovszky, Z. Excimer-laser processing of indium-tin-oxide films: An optical investigation. *J. Appl. Phys.* **1995**, *78*, 6211–6219.
- [25] Oh, M. S.; Hwang, D. K.; Lim, J. H.; Choi, Y. S.; Park, S. J. Current-driven hydrogen incorporation in zinc oxide. *Appl. Phys. Lett.* **2007**, *91*, 212102.
- [26] Leuchtner, R. E. Mass spectrometry and photoionization studies of the ablation of ZnO: Ions, neutrals, and Rydbergs. *Appl. Surf. Sci.* **1998**, *127*, 626–632.
- [27] Kwak, G.; Seol, M.; Tak, Y.; Yong, K. Superhydrophobic ZnO nanowire surface: Chemical modification and effects of UV irradiation. *J. Phys. Chem. C* **2009**, *113*, 12085–12089.
- [28] Lee, S.; Kim, W.; Yong, K. Overcoming the water vulnerability of electronic devices: A highly water-resistant ZnO nanodevice with multifunctionality. *Adv. Mater.* **2011**, *23*, 4398–4402.
- [29] Kwak, G.; Jung, S.; Yong, K. Multifunctional transparent ZnO nanorod films. *Nanotechnology* **2011**, *22*, 115705.
- [30] Jiang, X.; Jia, C. L.; Szyszka, B. Manufacture of specific structure of aluminum-doped zinc oxide films by patterning the substrate surface. *Appl. Phys. Lett.* **2002**, *80*, 3090–3092.
- [31] Kim, D. S.; Goesele, U.; Zacharias, M. Surface-diffusion induced growth of ZnO nanowires. *J. Cryst. Growth* **2009**, *311*, 3216–3219.
- [32] Fan, F. R.; Ding, Y.; Liu, D. Y.; Tian, Z. Q.; Wang, Z. L. Facet-selective epitaxial growth of heterogeneous nanostructures of semiconductor and metal: ZnO nanorods on Ag nanocrystals. *J. Am. Chem. Soc.* **2009**, *131*, 12036–12037.